REPORT DOCUMENTATION PAGE

Form Approved OMB NO. 0704-0188

1. REPORT DATE (DD-MM-YYYY)	2. REPORT TYPE	3. DATES COVERED (From - To)
13-06-2012	Final Report	1-Jul-2008 - 30-Jun-2011

4. TITLE AND SUBTITLE
Carbon Nanotube Array for Infrared Detection

5a. CONTRACT NUMBER
W911NF-08-1-0224

5b. GRANT NUMBER

5c. PROGRAM ELEMENT NUMBER
106011

6. AUTHORS
Jimmy Xu

5d. PROJECT NUMBER

5e. TASK NUMBER

5f. WORK UNIT NUMBER

7. PERFORMING ORGANIZATION NAMES AND ADDRESSES
Brown University
Office of Sponsored Projects
Brown University
Providence, RI 02912 -

8. PERFORMING ORGANIZATION REPORT NUMBER

9. SPONSORING/MONITORING AGENCY NAME(S) AND ADDRESS(ES)
U.S. Army Research Office
P.O. Box 12211
Research Triangle Park, NC 27709-2211

10. SPONSOR/MONITOR'S ACRONYM(S)
ARO

11. SPONSOR/MONITOR'S REPORT NUMBER(S)
54297-EL-DPS.1

12. DISTRIBUTION AVAILIBILITY STATEMENT
Approved for Public Release; Distribution Unlimited

13. SUPPLEMENTARY NOTES
The views, opinions and/or findings contained in this report are those of the author(s) and should not contrued as an official Department of the Army position, policy or decision, unless so designated by other documentation.

14. ABSTRACT
The core effort of this project has been the electrical transport and infrared photoresponse properties of carbon nanotube (CNT) systems.

15. SUBJECT TERMS

16. SECURITY CLASSIFICATION OF:			17. LIMITATION OF ABSTRACT	15. NUMBER OF PAGES	19a. NAME OF RESPONSIBLE PERSON
a. REPORT	b. ABSTRACT	c. THIS PAGE			Jingming Xu
UU	UU	UU	UU		19b. TELEPHONE NUMBER: 401-863-1439

Report Title

Carbon Nanotube Array for Infrared Detection

ABSTRACT

The core effort of this project has been the electrical transport and infrared photoresponse properties of carbon nanotube (CNT) systems.

Enter List of papers submitted or published that acknowledge ARO support from the start of the project to the date of this printing. List the papers, including journal references, in the following categories:

(a) Papers published in peer-reviewed journals (N/A for none)

Received Paper

TOTAL:

Number of Papers published in peer-reviewed journals:

(b) Papers published in non-peer-reviewed journals (N/A for none)

Received Paper

TOTAL:

Number of Papers published in non peer-reviewed journals:

(c) Presentations

Number of Presentations: 0.00

Non Peer-Reviewed Conference Proceeding publications (other than abstracts):

Received Paper

TOTAL:

Number of Non Peer-Reviewed Conference Proceeding publications (other than abstracts):

Peer-Reviewed Conference Proceeding publications (other than abstracts):

Received Paper

TOTAL:

Number of Peer-Reviewed Conference Proceeding publications (other than abstracts):

(d) Manuscripts

Received Paper

TOTAL:

Number of Manuscripts:

Books

Received Paper

TOTAL:

Patents Submitted

Patents Awarded

Awards

Graduate Students

NAME	PERCENT_SUPPORTED
FTE Equivalent:	
Total Number:	

Names of Post Doctorates

NAME	PERCENT_SUPPORTED
FTE Equivalent:	
Total Number:	

Names of Faculty Supported

NAME	PERCENT_SUPPORTED
FTE Equivalent:	
Total Number:	

Names of Under Graduate students supported

NAME	PERCENT_SUPPORTED
FTE Equivalent:	
Total Number:	

Student Metrics

This section only applies to graduating undergraduates supported by this agreement in this reporting period

The number of undergraduates funded by this agreement who graduated during this period:	0.00
The number of undergraduates funded by this agreement who graduated during this period with a degree in science, mathematics, engineering, or technology fields:.....	0.00
The number of undergraduates funded by your agreement who graduated during this period and will continue to pursue a graduate or Ph.D. degree in science, mathematics, engineering, or technology fields:.....	0.00
Number of graduating undergraduates who achieved a 3.5 GPA to 4.0 (4.0 max scale):	0.00
Number of graduating undergraduates funded by a DoD funded Center of Excellence grant for Education, Research and Engineering:	0.00
The number of undergraduates funded by your agreement who graduated during this period and intend to work for the Department of Defense	0.00
The number of undergraduates funded by your agreement who graduated during this period and will receive scholarships or fellowships for further studies in science, mathematics, engineering or technology fields:	0.00

Names of Personnel receiving masters degrees

NAME

Total Number:

Names of personnel receiving PHDs

NAME

Total Number:

Names of other research staff

NAME PERCENT_SUPPORTED

FTE Equivalent:

Total Number:

Sub Contractors (DD882)

Inventions (DD882)

Scientific Progress

Technology Transfer

Carbon Nanotube Array for Infrared Detection

Final Report

Jimmy Xu
Professor of Engineering and Physics,
Division of Engineering, Box D
Brown University
Providence, RI 02912
401-863-1439
Jimmy_Xu@Brown.edu

Report date: 09/28/2011
ARO Proposal Number: 54297-EL-DPS
Agreement Number W911NF-08-1-0224
Managed by: Dr. Bill Clark, ARO Electronics Division Chief

Table of Contents:

List of Figures:

1. Introduction

The core effort of this project has been the electrical transport and infrared photoresponse properties of carbon nanotube (CNT) systems. The word "system" is important in the context of our work because we have focused on the properties of materials and devices consisting not of a single CNT, but of assemblies with large numbers of CNTs. In these systems it is often not only the properties of single CNTs that count, but also (and primarily) the way in which they interact with each other and with the other materials comprising the system. Thus a rich interplay between such properties ensues that has been able to generate materials and devices with unprecedented functionality and with rich and interesting electronic properties.

Two cases illustrate this. The first is the system that we investigated in the earlier parts of this effort consisting of a macroscopically ordered array of CNTs, all which formed individually electronic-grade heterojuctions with an underlying silicon substrate. This system is comprised essentially of billions of individual CNTs connected in parallel. As such, the properties of individual CNTs were just as important as those of their interaction with each other (cross-talk) and with the other elements of the system. For example, a few dozens of shorts within this billion or so of parallel diodes could potentially render the device useless. Yet, our development of novel sample fabrication and CNT growth strategies made such shorts a non-issue. This allowed us to demonstrate and study the interesting electrical rectification properties of this CNT-Silicon heterojunction system, and led to the discovery that this system could behave as a broad-band detector of infrared radiation, capable of operating in both cooled and uncooled modes. A further extension of this system was then achieved by loading the interior spaces of the CNTs with other materials of interest, including lead sulfide in both quantum dot and nanowire forms.

The second illustrative system was the one obtained in the latter parts of the effort and consisting of a composite material consisting of CNTs dispersed within a thermoresponsive polymer. Here the

properties of the interaction between CNTs really came forth, and led to the observation of unsurpassed thermotransduction capability, with world-record temperature coefficients of resistance (TCR) in excess of -40 %/^{o}C near room temperature. This amazing finding came in stark contrast to the heterojunction system described above. Here the electrical transport properties are determined almost entirely by the interaction between CNTs. The CNTs, which form a random network in the polymer matrix, serve as "tunneling hubs" for the electrons as they move across the network. The network resistance is determined by the tunneling of electrons between hubs (CNTs) in the network. As such, the electronic transport properties of this system are quantum mechanical in nature. It thus consists of a macroscopic embodiment of the quantum tunneling process. With the added thermoresponsivity of the polymer, this system unraveled a novel strategy for achieving unprecedented sensitivity, i.e. combining a stimulus-responsive polymer with a network of quantum resistors, which has led, among others, to a patent application.

It would be both a daunting and repetitive task to survey here all the work that has been done in this effort. The systems are already described in detail in the previous interim reports and in the almost twenty publications that have emerged from and in connection with this effort. We thus refer to the list of publications of this effort, given below, for further details. As such, we will focus here only on the latest developments, and discuss further explorations with the systems developed so far and with novel systems and material platforms as well. We begin with a review of the CNT-PNIPAm composite system and its world-record breaking TCR. This material has recently been submitted for publication and was the subject also of a recent patent application. We will describe the system and its mechanisms in some detail, its current and future potential applications and our future research plan with relation to it.

2. Giant thermotransduction in CNT-polymer nanocomposites

2.1 Description of the system

Bolometric infrared responses occur in many natural systems and now increasingly in man-made infrared sensing devices. In contrast to photocarrier generation across a band gap, nature's bolometers convert infrared radiation into heating of tissues thereby inducing thermotransduction. They can achieve extraordinary sensitivity without requiring cryogenic cooling. One well-known example is found in pit vipers in the form of a thin sensory membrane suspended above an air chamber. [1, 2] The pit membrane is connected mechanically and electrochemically to nerve branches and is highly vascular to allow fluidic cooling after stimulation and removing afterimages. Despite remarkable advances in materials for uncooled bolometric sensing, the natural counterparts are still far superior in both sensitivity and speed. We report a progress in the pursuit of improving man-made bolometric materials. Giant temperature coefficients of resistance are achieved in a carbon nanotube composite with a phase-change polymer that dynamically modulates charge transport. Enhanced bolometric response to infrared illumination is also observed.

The temperature coefficient of resistance (TCR) is a key figure-of-merit for man-made bolometric devices. In recent years, intensified interest in uncooled IR sensing and the search for high TCR materials have led to the development of the vanadium oxides, [3] which display near-room-temperature TCR values of ~ -3 %/^{o}C. [4] Other materials exhibiting metal-to-insulator phase transitions that achieve double-digit TCR values near the transition point have also been investigated. [5, 6] High TCR is, however, not the only important parameter for bolometric sensing. Heat capacity, thermal conductivity, mechanical strength, and infrared absorption efficiency are also important. [7] In these regards, thin membranes of carbon nanotubes have much to offer. Carbon nanotube membranes display strong and broad-band optical absorbance, which enables detection over broad spectral ranges. [8] Their electrical and thermal conductivities can be tailored to specific requirements by appropriate selection of carbon nanotube type such as metallic or semiconducting (and ratios thereof), multi-walled, or even semi-amorphous or doped nanotubes. [9] In addition, carbon nanotube membranes are known to have large strength-to-weight ratios, [10] which facilitates the fabrication of standalone suspended thin films that are needed for heightened heat sensitivity. However, the highest reported TCR values for carbon nanotube

membranes and carbon nanotube nanocomposites are still in the neighborhood of -0.5 %/°C near room temperature. [11-14] Such relatively low TCR limit the usability of carbon nanotube materials in bolometric infrared sensing, and intensify the requirements for thermal management and device engineering in order to achieve adequate responsivity.

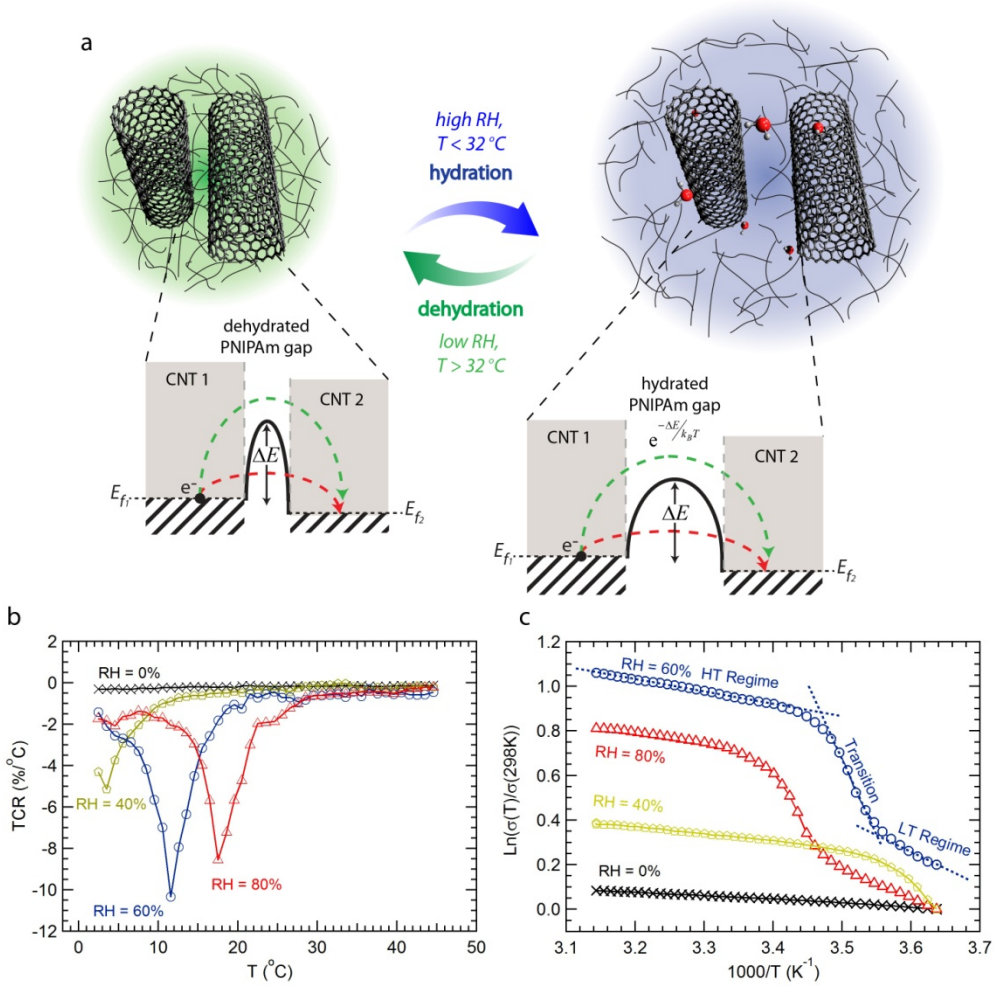

Figure 1. Enhanced TCR and conductivity response via phase change. (a) Schematic illustrating the effects of hydration on the intertube spacing in and the intertube electron tunneling potential barrier. (b) Temperature behavior of the TCR at various relative humidity levels. (c) Temperature behavior of the conductivity (normalized to the value at 45 °C at various relative humidity levels. The curve corresponding to 60% relative humidity is offset vertically for better viewing. The dashed lines serve as a

guide to the eye in identifying the different regimes discussed in the text. The thickness of the film was measured by AFM to be ~ 500 nm.

Because of the high conductivity of individual carbon nanotubes, the electrical resistance across a carbon nanotube membrane is determined by the tunneling of electrons across the gaps that exist between nanotubes. [15] Such resistances are quantum mechanical in nature; [16-18] they depend exponentially on the temperature and the parameters describing the tunneling gaps, in particular the tunneling gap width. We leverage on such exponential dependence by incorporating into the nanotube membrane a non-conductive phase-changing polymer that exhibits large dynamic changes in volume with temperature. The resulting changes in the intertube gaps with temperature dynamically modulate the resistance of the nanotube-polymer network, and results in large TCR values. The polymer, poly(N-isopropylacrylamide) (PNIPAm), was chosen for its near room temperature (T_C ~ 32 ^oC) hydrophilic-to-hydrophobic phase-transition. [19] In the hydrophilic state, below T_c, PNIPAm can interact with moisture present in the surroundings and expand in volume by as much as one order of magnitude as a result of hydration. [20] At higher temperatures, PNIPAm expels its moisture content and shrinks in volume. These effects are illustrated in Figure 1 (a).

Figures 1 (b) and (c) show the temperature behavior of the TCR and conductivity of the carbon-nanotube-PNIPAm nanocomposite. As the temperature is decreased below 32 ^oC, the nanocomposite transitions into the hydrophilic state. This enables it to interact with the water vapor present in the atmosphere within the measurement chamber. For sufficiently high relative humidity values, the hydration and swelling of the nanocomposite resulted in large changes in the conductivity, with observed TCR values several times greater than those in previous reports on carbon nanotube composites. [11-13, 21] For example, the film measured in Figure 1 achieved TCR values in excess of -10 %/^oC. Measurements of films that were suspended across an air gap yielded TCR values as large as -40 %/^oC, as shown in the Section 2.2 below. The suspended films achieved larger TCR because of the larger contact

surface with the humid atmosphere. In most cases a peak was observed in the TCR as a function of temperature. The temperature at which this peak occurred was found to correspond with the dew point temperature of water for the given conditions of relative humidity and temperature. When the relative humidity was sufficiently low, only relatively small TCR were obtained, with values comparable to those in prior reports on carbon nanotube composite materials. [11-13, 21]

The observed temperature and humidity behavior of the TCR can thus be understood in terms of two separate but intimately related changes that occur in the nanocomposite as a function of temperature. The first corresponds to the phase transition in the polymer's hydrophilicity. As discussed above, this transition occurs at temperatures close to 32 ^{o}C. [19] The second is the change in volume that results from hydration/dehydration of the nanocomposite. This latter change requires a supply of water molecules, which in our measurement setup occurs via the interaction with humidity in the atmosphere. As such, the largest TCR values are observed at the dew point, where the onset of condensation provides a virtually limitless supply of water, and not at 32 ^{o}C as one might initially expect. We note, however, that although the observed TCR peaks occurred at the dew point, enhanced TCR values were also observed at temperatures several degrees above the dew point, as seen in Figure 1 (c). The photoresponse of the membrane conductivity also showed similar behavior as discussed below.

The near-room-temperature conductivity σ of carbon nanotube composites with non-conductive polymers is well described by a thermal activation model, given by equation (1), [17, 22-25] where T_0 is an activation temperature that depends on the tunneling barrier parameters. In particular, if a homogeneous dispersion of nanotubes in the polymer is assumed, T_0 is found to be directly proportional to the mean intertube distance *w*. Here *w* (and hence T_0) may also depend on the temperature via the thermal expansion of the polymer. Additionally, in our nanocomposites, we expect *w* to depend on the relative humidity, which greatly influences the swelling of the polymer as discussed above.

$$\sigma = \sigma_0 e^{-T_0/T} \tag{1a}$$

$$T_0 \sim w(T, RH) \tag{1b}$$

When applied to our system, the model in equation (1) reveals two static regimes with constant T_0. We label these the high temperature (HT) and the low temperature (LT) regimes, as indicated in Figure 1 (c). In the HT regime the nanocomposite is hydrophobic and shrunken. This is reflected in the relatively small values of T_0 that suggest narrow tunneling barriers according to equation (1b). In contrast, in the LT regime the nanocomposite is hydrated and swollen. This results in larger tunneling barriers and larger T_0. At 80% relative humidity T_0 increased from ~ 500 K in the dehydrated HT regime to more than 1500 K in the hydrated LT regime. The actual swelling process occurs in the transition region connecting the LT and HT regimes. In this region T_0 assumes its largest value (~ 5000 K) and becomes temperature dependent. Such dependence results in a nonlinear behavior in the semi-logarithmic plot of the conductivity vs. temperature, and indicates dynamically changing tunneling barriers as a function of temperature. The peak in the TCR noted above occurs in the transition region.

The hydration process is governed by diffusion of water vapor from the surrounding atmosphere into the nanocomposite, followed by incorporation of the water molecules into the hydrogel structure and swelling. [26] In the HT regime, these processes must compete with repulsion forces from the hydrophobic polymer molecules. At lower temperatures, however, the changes in polymer conformation resulting from the hydrophobic-to-hydrophilic phase transition act favorably to incorporate water into the nanocomposite structure. Under these conditions, the swelling process is regulated by the supply of water. The constant T_0 observed at temperatures below but relatively close to the dew point of water in Figure 1 (c) also suggests that the hydration process quickly reaches saturation. For lower temperatures the nanocomposite no longer swells and settles into the LT regime with constant thermal activation energy.

Figure 2 shows the photoresponses of the nanocomposite resistance obtained at different relative humidity levels as a sample of the nanocomposite was illuminated with light from an infrared light emitting diode (880 nm, ~10 mW/cm^2). At 0% relative humidity, the relative change in resistance as a function of illumination $\Delta R/R$ was only ~ -0.1% and the TCR remained below ~ -0.3 $\%/^oC$. These values are comparable with those reported on other works on carbon nanotube nanocomposites. [11-13] When the relative humidity was increased, however, partial or complete hydration of the nanocomposite was

possible, and the same mechanism described above and responsible for the increased TCR now led to enhanced thermotransduction and thus to enhanced photoreponses. As seen in Figure 2, ΔR/R gradually increased for relative humidity values between 0% and 70%. At 70 % relative humidity ΔR/R became grater that -6% while the observed TCR was greater than -15 %/^{o}C. Both of these figures correspond to an enhancement of approximately fifty times compared with the dehydrated values.

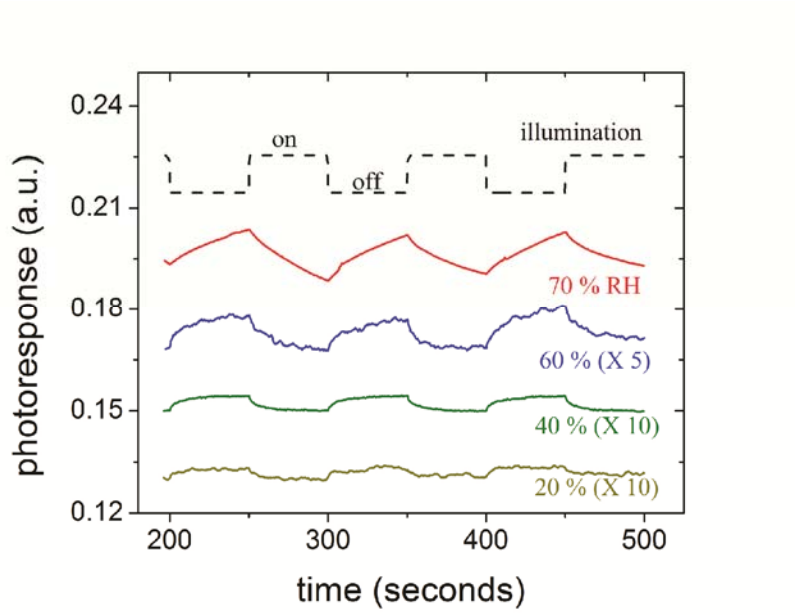

Figure 2. Bolometric response of carbon nanotube-PNIPAm nanocomposites. The bolometric response is measured at various relative humidity levels with a sample temperature of 15 ^{o}C. The amplitudes of the photoresponse for relative humidity of 60% and below are magnified for better viewing. The magnification is indicated in the parentheses.

As shown in Figure 3, both the photoresponse and the TCR exhibited very similar behavior as a function of relative humidity and temperature. The photoresponse time constant, τ, was also observed to vary similarly to the TCR, albeit with much smaller enhancement near the dew point. This behavior is expected because the incorporation of moisture in the nanocomposite also increases its heat capacity. [7]

For bolometric sensors, τ can be written in the familiar form $\tau = RC$, where C is the heat capacity of the sensing element and R is the total thermal resistance that couples the sensing element to its surroundings. The dependence of the photoresponse on the TCR and the relatively large time constants observed under all measurement conditions are consistent with the photoresponse being bolometric in nature. Measurements of the photoresponse with chopped light are also in agreement with this finding, as discussed in section 2.2. Figure 3 also shows the changes in the electrical resistance of the sample. We note that the photoresponsivity in thin film bolometers is known to be proportional not only to the TCR but also to the nominal value of the resistance of the bolometer sensing element. [7] As seen in Figure 3, however, the observed increase in photoresponse was typically over one order of magnitude greater than the corresponding increase in resistance.

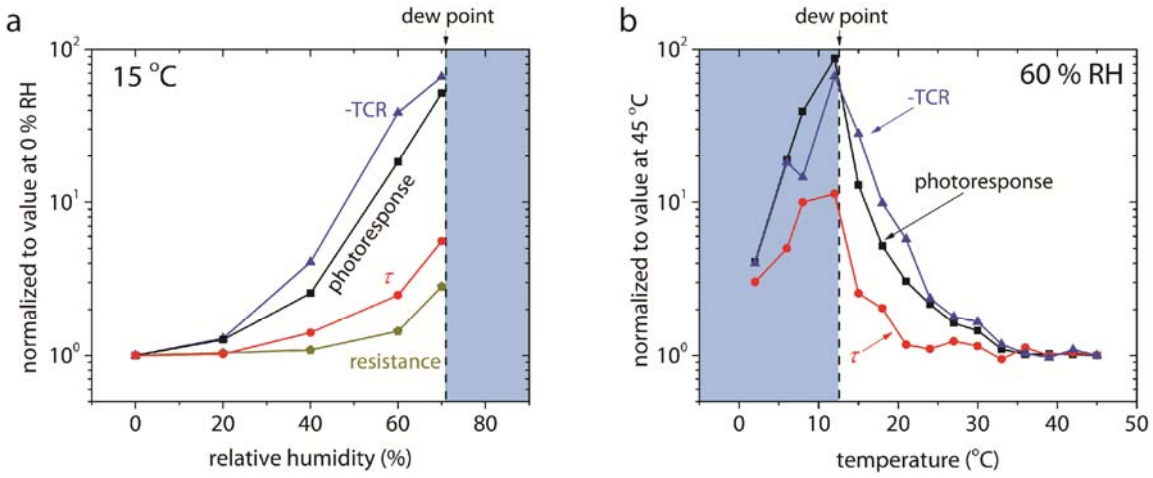

Figure 3. Photoresponse dependence on relative humidity and temperature. (a) Relative humidity behavior of the photoresponse, TCR, electrical resistance and τ measured at 15 ^{o}C. The data are normalized to the value at 0% RH and the dashed line indicates the dew point relative humidity. (b) Temperature behavior of the photoresponse, TCR, and τ at 60% relative humidity. The data are normalized to their values at 45 ^{o}C and the dashed line indicates the dew point temperature.

In summary, a carbon nanotube-polymer nanocomposite that changes its electrical resistivity by as much as -40% in response to a one-degree change in temperature is achieved in a carbon nanotube

membrane via incorporation of a phase-change polymer medium. In a similar context to the system studied here, other temperature sensitive polymers, especially ones exhibiting phase-transition behavior (or glass transitions) may be explored and may offer alternatives in cases where humidity sensitivity may be undesirable. Combining the lightweight, high mechanical strength and high optical absorbance of carbon nanotubes with the potential of built-in vascular cooling, these nanotube-polymer composites incorporate a novel sensing paradigm, i.e. that of introducing large dynamic phase-changes into a network of “quantum tunneling” resistors, and may in the context presented here hold promise as a platform for enhanced uncooled infrared imaging.

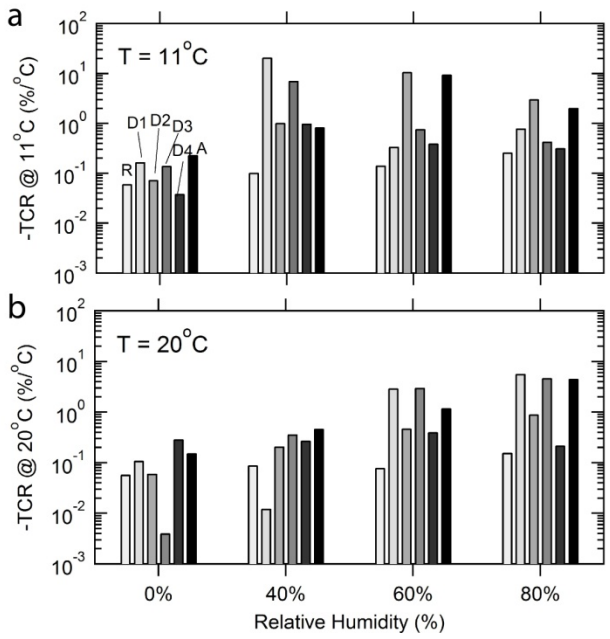

Figure 4. TCR at various relative humidity levels for two distinct device temperatures.

2.2. Methods of fabrication

Carbon nanotube (CNT)-PNIPAM nanocomposite film synthesis

Thin-film samples of CNT-PNIPAM composite were prepared either by filtration or by drop casting a desired amount of an aqueous solution of CNTs and PNIPAM onto porous alumina substrates (Anodisk, Whatman) and allowing the solution to dry under room temperature and pressure conditions. The water-dispersed CNTs containing 1% sodium dodecyl sulfate (SDS) (Nano-Integris) were dissolved in an aqueous solution of PNIPAM (Sigma-Aldrich) containing 1% SDS (Sigma-Aldrich). The compositions of various samples prepared and tested are given in Table 1. This method resulted in highly uniform nanocomposite films without any observable bundling of CNTs or aggregations of polymer, as seen in Figure 5. The latter were confirmed by both scanning electron microscope (SEM) and atomic force microscope (AFM) imaging of the samples. After film formation, contacts were made to the samples either by masked electron beam evaporation of Pd or by attaching wire contacts directly to the films with silver paste. Both methods yielded similar results.

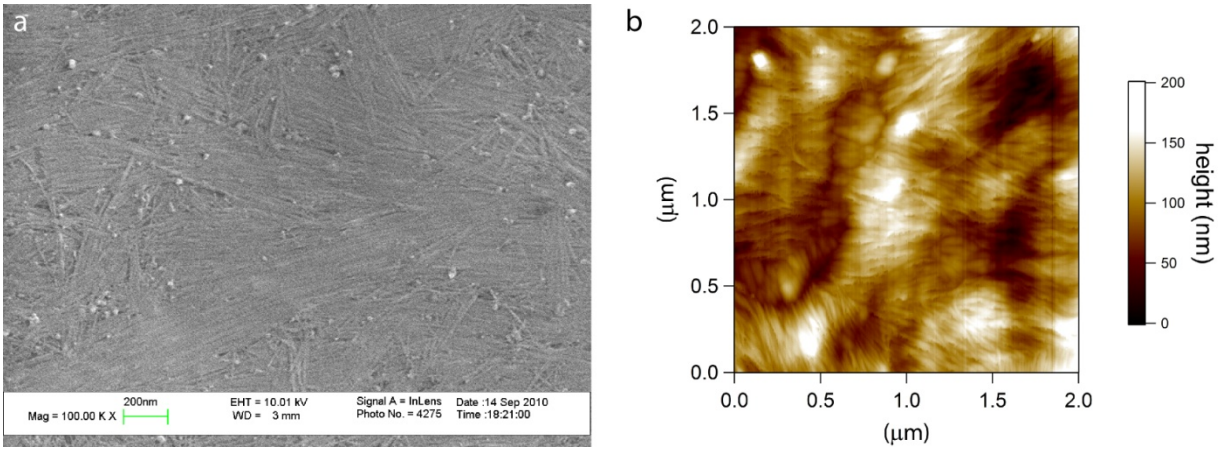

Figure 5. Uniformity of dispersion of CNTs in the CNT-PNIPAM nanocomposites. (a) SEM and (b) AFM images of the surface of a CNT-PNIPAM sample (sample D4 in table S1).

Table S1 – Nanocomposite Samples of CNT-PNIPAM

Sample	Description	Composition	CNT mass fraction
R	CNT film, ~ 10 nm thick	1 ml (0.005 mg/ml) CNT	1
A	CNT-PNIPAM film	1 ml (2.5 mg/ml) CNT + 1 ml (50 mg/ml) PNIPAM	0.05
D (1-4)	CNT-PNIPAM films with varying CNT mass fraction	D1 – 1 ml (0.001 mg/ml) CNT + 1 ml (10 mg/ml) PNIPAM D2 – 1 ml (0.002 mg/ml) CNT + 1 ml (10 mg/ml) PNIPAM D3 – 1 ml (0.005 mg/ml) CNT + 1 ml (10 mg/ml) PNIPAM D4 – 1 ml (0.01 mg/ml) CNT + 1 ml (10 mg/ml) PNIPAM	D1-10^{-4} D2-$2x10^{-4}$ D3-$5x10^{-4}$ D4-10^{-3}

TCR measurement

A schematic of the measurement setup is given in section 2.2. The sheet resistances of the samples were measured in a sealed environmental chamber kept at room temperature (~ 22 ^{o}C) and 1 atm. The relative humidity value inside the measurement chamber was controlled by adjusting the flow of wet and dry N_2 (wet N_2 was obtained by flowing dry N_2 through a water bubbler) and monitored with a hygrometer. The samples were mounted on a thermoelectric heater/cooler plate inside the chamber. Sheet resistance measurements were taken at sample temperatures between 2 and 45 ^{o}C in increments of 1 ^{o}C. A source measure unit (Keithley 236, Keithley) was used for the electrical measurements in two probe mode and a semiconductor parameter analyzer (HP 4145B, Hewlett Packard) was used for the four point probe measurements. The sample temperature was adjusted and controlled via a temperature controller (LDC 3722B, ILX Lightwave) and monitored by a thermocouple that was mounted onto the Al block that served as sample stage in the chamber (see figure 6). Each set temperature was allowed to stabilize for 2

minutes before the measurement was taken. Our initial testing revealed that both four and two-point probe methods yielded similar results, indicating that contact resistances were negligible. The TCR (in %/^{o}C) was calculated from the measured resistance data according to equation 2. Several samples made with similar composition were tested and all showed similar results.

$$\frac{TCR}{\left(\%/^{o}C\right)} = \frac{100}{R}\frac{\Delta R}{\Delta T} \tag{2}$$

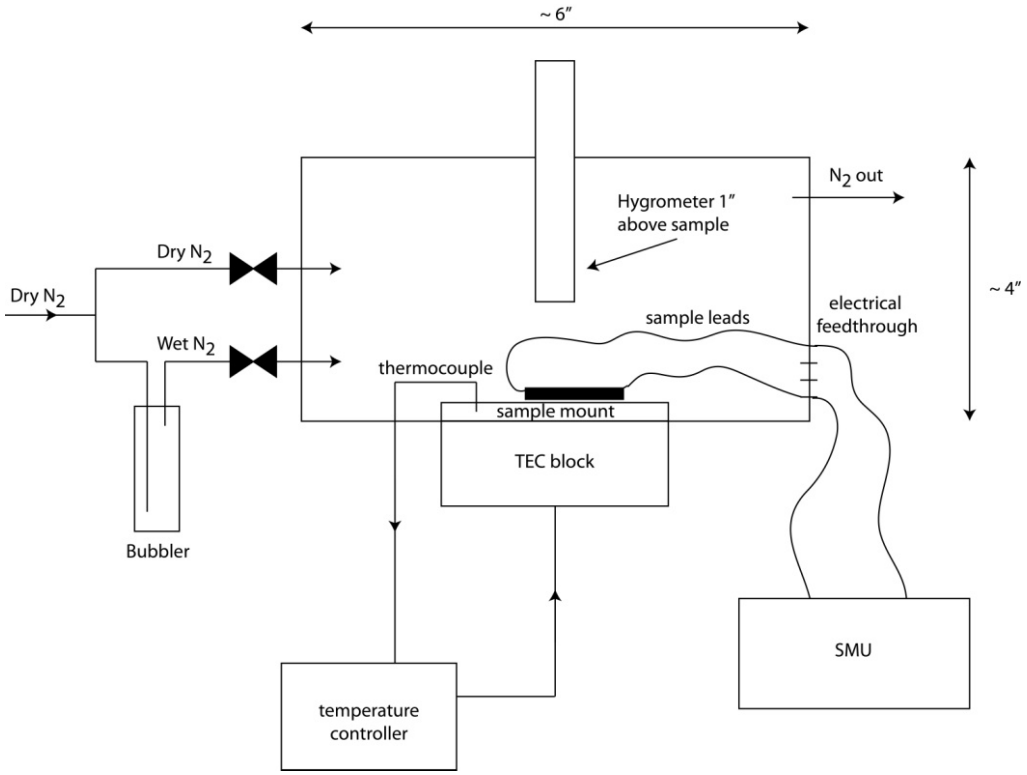

Figure 6. Schematic of the temperature and humidity controlled measurement chamber. The sample chamber is sealed to prevent contact with the external atmosphere in the room. The relative humidity in the atmosphere inside the chamber is regulated by flow of wet and dry N_2.

Dependence on CNT mass fraction

As discussed by Connor et al [25] and references therein, Equation 1 can be written in the form $\ln \sigma \propto -w$. In terms of the sheet resistance (or the resistivity), it is equivalent to $\ln R_{sheet} \propto w$. For a homogeneous dispersion of CNTs in the PNIPAm host medium, the gap width w and the CNT mass fraction p are related as $w \sim p^{-1/3}$. Therefore we have

$$\ln R_{sheet} \propto p^{-1/3}. \quad (3)$$

Figure 7 (a) shows the dependence of the sheet resistance on the temperature for nanocomposite sample with different CNT mass fraction (samples D1-D4 on Table 1). The measurement was conducted at 60 % relative humidity. The CNT mass fraction is indicated above each curve. The temperature behavior is consistent with the discussion in the main text. Below 15 ^{o}C the sheet resistance experiences a sharp increase due to the hydration of the polymer. The relative amount by which the sheet resistance increases becomes larger as the CNT mass fraction decreases. This behavior is expected because a relatively larger number of conduction paths are disrupted in the nanocomposites with smaller CNT mass fraction as the polymer expands. Figure 7 (b) shows the same data plotted as a function of CNT mass fraction. The lines are linear fits to the data points. The relation in Equation 2 is seen to be obeyed. Only at low temperatures and low CNT mass fraction does the relationship appear to not hold. This is illustrated by the data point corresponding to 5 ^{o}C for sample D1, which seems to fall abnormally above the other points. A linear fit to the data at 5 ^{o}C including this last data point yields the dashed blue line, which clearly deviates from the others.

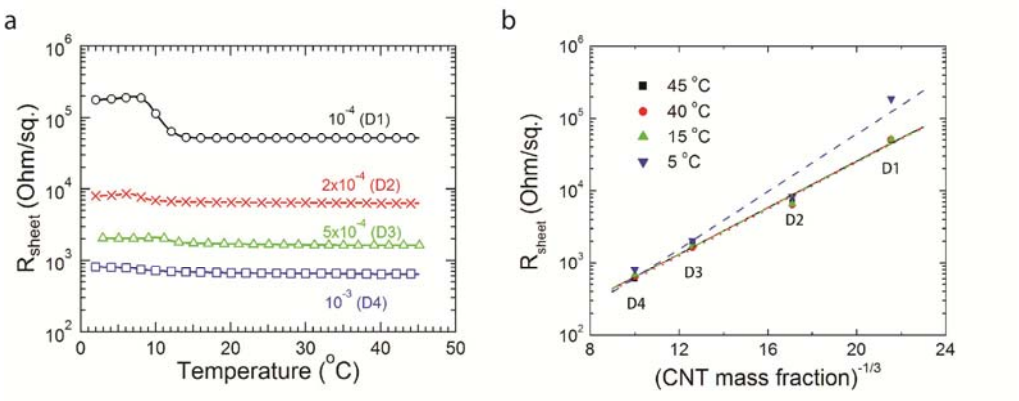

Figure 7. Verification of the relation in equation (3). (a) Sheet resistance as a function of temperature and (b) sheet resistance as a function of carbon nanotube mass fraction for samples D1-D4 in table S1.

Photoresponse measurement

Films with the composition of sample A in table 1 (3 mm by 3 mm and 1 μm thick) were suspended across an air gap of ~ 0.3 mm between two glass slides that were previously coated with 200 nm of palladium. The suspended films were ~3 mm by 3 mm and 1 μm thick. Electrical contacts were made to the Pd coated glass without disturbing the films. The photoresponse was measured at constant current by measuring the voltage drop across the films with a source measure unit (Keithley model 236). Illumination was provided by an infrared light emitting diode (LED, wavelength 880 nm) at a power density of 10 mW/cm^2. The measurements were performed at room pressure with the atmosphere in the environmental chamber kept at a constant temperature of 22 ^{o}C. The sample temperature was controlled independently.

A schematic of the device prepared for measuring the photoresponse is shown in Figure S5. Frequency modulation measurements were performed by chopping the LED light and measuring voltage drop across the sample at fixed current DC bias with a lock-in amplifier (Stanford Research Systems, model SRS 830). Data in Figure S5 corresponds to the sample measured in Figure 3 of the main text. Figure S5 (a) shows the behavior of the photoresponse as a function of modulation frequency of the

source. The strong decay of the photoresponse intensity is a characteristic of bolometric response. The TCR and resistance data at two relative humidity values are shown in Figure S5 (b).

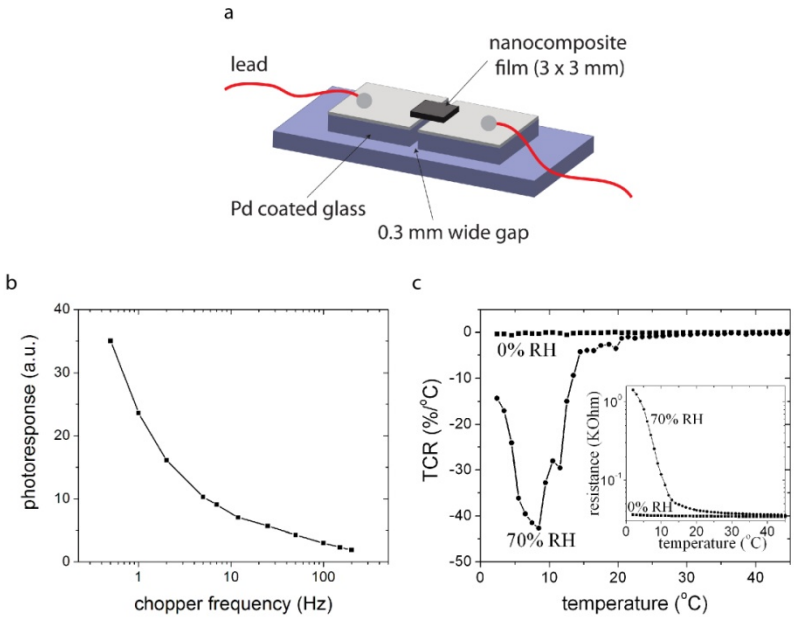

Figure 8. Chopped light measurements and TCR for suspended nanocomposite film. (a) Frequency dependence of the photoresponse under chopped illumination. The measurement was performed at 40% relative humidity. (b) Temperature dependence of the TCR and resistance (inset).

3. Future prospects

3.1 – Development of a CNT-PNIPAm IR "Webcam"

We have begun efforts to extend this platform to a focal-plane array interfaced by its own independent, low-cost electronics. In this early stage of development, we have built a simple "proof-of-concept" prototype that works from its own electronic circuitry and reads and displays the infrared intensity on a single element CNT-PNIPAm detector, as shown in Figure 9. We hope in the continuation of this effort to extend this platform to a multi-pixel focal plane array and establish a computer interface, where the resulting device would operate as a low-cost (possible an order of magnitude cheaper than commercial alternatives) broadband infrared "webcam". The lower cost is enabled in principle by the CNT-PNIPAm platform, which lends itself to much easier fabrication and simpler processing strategies

than the current competing platforms (these are either the vanadium oxide uncooled bolometers that require intricate fabrication techniques or the small band-gap semiconductors, which require expensive crystalline materials, such as lead selenide, and are hampered by the need of cryogenic cooling for noise reduction).

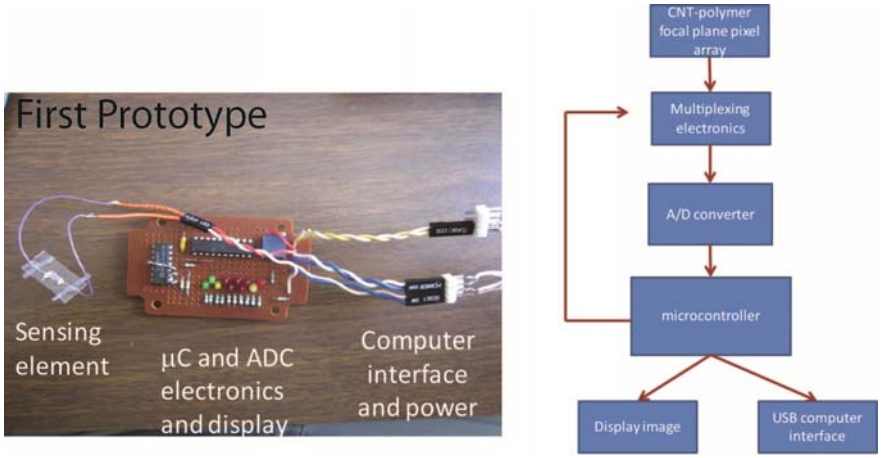

Figure 9. First prototype of CNT-PNIPAm device. The aim is to eventually develop a low cost, lightweight and portable "webcam" broadband IR detector.

Another great advantage of this platform is its mechanical properties. Carbon nanotube membranes are known to have large strength-to-weight ratios, [10] which facilitates the fabrication of standalone suspended thin films that are needed for heightened heat sensitivity in bolometers. In addition, these properties open the possibility for flexible (bendable), surface conformal, or even wearable detectors. Such properties are not available in current semiconductor-based technologies because the materials are brittle, which leads to cracking and changes in the electrical properties if bent. Such characteristics of CNT films are already bring about changes in the way we think about electronic components, and have played a role, e.g. in flexible display technology.

In order to enable the implementation of such flexible and scalable CNT detectors, methods of processing, patterning (lithography), thermal isolation, and electrical interfacing must be developed. This, together with the development of an electronic platform that is compatible with this philosophy, and thus

meets the requirements of simplicity, functionality, low-cost and low environmental footprint are part of what we propose to develop in this effort. Thus, methods strategies for processing composite films from their raw, as-produced form to make them compatible with the requirements for bolometer devices, including proper thermal isolation, electrical interfacing, and compatibility with on-board electronic components will be developed in this effort.

3.2. Extending the principle of phase-change within a CNT random network to other areas of impact

The principles behind the extraordinarily high responsivity of the CNT-PNIPAm platform described in section 2 are much more far reaching than their applications in IR sensing. We recognize that there are two key factors enabling such magnified responses. First is the exponential dependence of the tunneling probability on the spacing (or the medium) between CNTs. Second, is the dynamic change in this spacing brought about by the volume-phase change in the polymer. These two principles provide us with a paradigm shift in terms of sensing strategies because they can be extended to other platforms targeting sensing that may or may not be temperature related. These may include, besides temperature, the pressure, pH levels, light, and even ultrasound. Some of these have already been demonstrated in our preliminary studies but need further investigation before publication. They include sensitivity to

- pressure (touch)
- microwave
- ultrasound
- organic solvents

Others remain of particular interest, such as the sensing of changes in pH, as described below. Some possible applications and extensions of this platform are described in Figure 10.

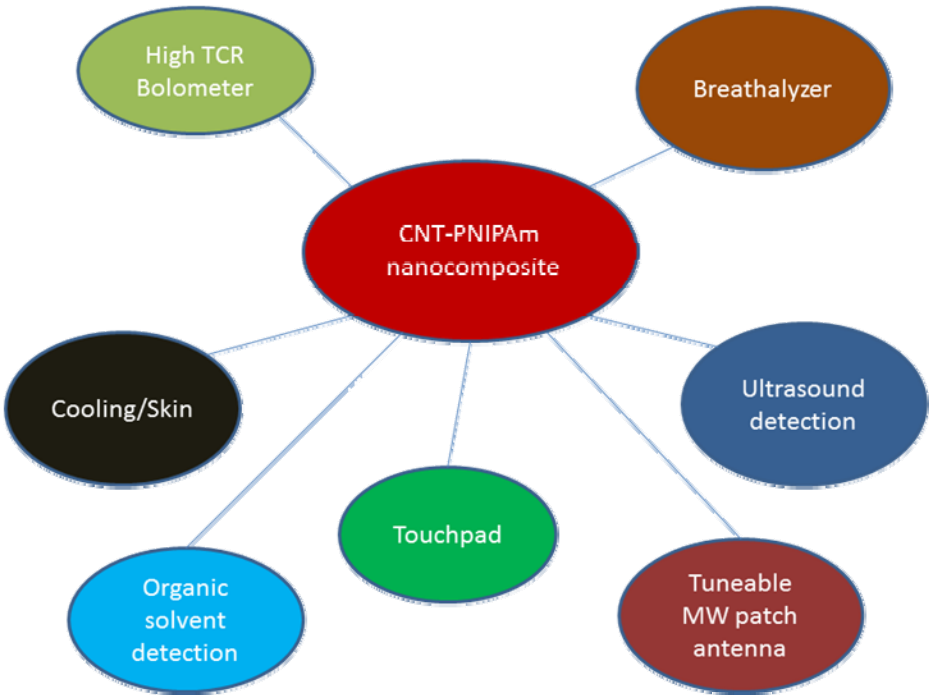

Figure 10. Some possible platforms extending the concept of a phase change induced responsivity in a network of CNTs.

Of the platforms listed in Figure 10, one of particularly high interest is the sensing of pH. Many chemical reactions are accompanied by changes in pH and could in principle be studied by monitoring the electric current through a composite of CNTs with a pH sensitive polymer. Polymers exhibiting changes in volume and/or conformation as a function of pH are available, although their composites with CNTs have not yet been investigated. This opens the possibility for magnified response to changes in pH by the pH induced volume changes in the polymer, similar to the temperature induced volume changes described in section 2. Of particular interest among the pH sensing applications is the monitoring of sugar levels in diabetes patients. Sugar levels can be detected via the reaction of the glucose oxidase protein with glucose, which results in a decrease of the pH through the production of hydrogen peroxide. The monitoring is traditionally done by measuring the conductivity of blood droplets reacted with glucose

oxidase. However, breath sensing of body-glucose levels has been investigating in a number of studies before. In some cases trained dogs have been capable of detecting and warning patients of high glucose levels by simply sniffing the patient's breath. By mixing CNTs with a pH sensitive polymer, particularly one that changes volume accompanying a change in pH, we will seek to obtain a CNT network whose resistivity is determined by the amount of glucose in the breath exhaled upon it. By functionalizing this material with glucose oxidase enzymes we will seek to obtain a material that, in appropriate form, will detect small changes in pH induced by breathing on it, such that the glucose present in the breath will react with the oxidase and cause changes in the resistance that are magnified by the volume expansion of the polymer.

List of Publications

1. G. E. Fernandes, J. H. Kim, A.K.Sood, and J. Xu, "Giant thermotransduction through phase change in carbon nanotube polymer nanocomposites", (submitted to Nature Nanotechnology).
2. G. E. Fernandes, M. B. Tzolov, J. H. Kim, Z. Liu, and J. Xu, "Infrared Photoresponses from Filled Multi-Wall Carbon Nanotubes", J. Phys. Chem. C, 114, 22703–22709, (2010).
3. G. E. Fernandes, Z. Liu, J. H. Kim, C.-H. Hsu, M. B. Tzolov, and J. Xu, "Quantum Dot/Carbon Nanotube/Silicon Double Heterojunction for Multi-Band Room Temperature Infrared Detection", IOP Nanotechnol., 21, 465204, (2010).
4. R. Osgood III, S. Giardini, J. Carlson, B. Kimball, M. Hoey, G. E. Fernandes, Z. Liu, J. H. Kim, J. Xu, and W. Buchwald, "Coupled, large-area gold nanowire arrays for nanorectenna energy conversion", Paper 7757-39, SPIE Proceedings Vol. 7757, (2010).
5. A. K. Sood, R. A. Richwine, Y. R. Puri, T. Manzur, N. K. Dhar, D. L. Polla, P. S. Wijewarnasuriya, Y. Wei, J. Zhou, C. Li, Z. L. Wang, G. Fernandes, J. M. Xu, "Next generation

nanostructure-based EO/IR focal plane arrays for unattended ground sensor applications", SPIE Proceedings, Vol. 7693, (2010).

6. A. K. Sood, R. A. Richwine, Y. R. Puri, G. Fernandes, C.-H. Hsu, J. H. Kim, J. Xu, N. Goldsman, N. K. D. Priyalal, S. Wijewarnasuriya, B I. Lineberry, "Design and Development of Carbon Nanostructure based Microbolometers for IR Imagers and Sensors", Proceedings of the SPIE /DSS conference in Orlando, SPIE Proceedings Vol. 7679, (2010).

7. G. E. Fernandes, J. H. Kim, Z. Liu, J. Shainline, R. Osgood III, J. Xu, "Using a forest of gold nanowires to reduce the reflectivity of silicon", Opt. Mater., 32, 5, 623-626, (2010).

8. R. Osgood III, M. Hoey, B. Kimball, J. Carlson, D. Ziegler, G. E. Fernandes, Z. Liu, J. H. Kim, and J. Xu, "Coupled, large-format gold nanowire arrays for nanorectenna energy conversion", SPIE, 2010.

9. Z. Liu, J. H. Kim, G. E. Fernandes, and J. Xu, "Room temperature photocurrent response of PbS/InP heterojunction", Appl. Phys. Lett. 95, 231113 (2009).

10. R. Osgood III, J.B. Carlson, B.R. Kimball, D.P. Ziegler, J.R. Welch, L.E. Belton, G. Fernandes, Z. Liu, J.M. Xu, "Plasmonic nanorectennas for energy conversion", SPIE, 2009.

11. T.-F. Kuo, M. B. Tzolov, D. A. Straus, and Jimmy Xu, "Electron transport characteristics of the carbon nanotubes/Si heterodimensional heterostructure", Appl. Phys. Lett., 92, 212107, 2008.

12. Jimmy Xu, "Formation and infrared sensing of highly ordered carbon nanotube - silicon heterojunction arrays", June 12, 2008, Army Natick Soldier Research Development and Engineering Center, Natick, MA

13. Jimmy Xu, "Carbon Electronics", MIGAS 2008, Autrans, France, June 28-July 4, 2008.

14. Jimmy Xu, "Carbon Nanotube – Silicon Heterojunction Diode and IR applications", ESSDERC-ESSCIRC 2008, Edinburgh, UK, Sept 17-20, 2008

15. M. B. Tzolov, T.-F. Kuo, D. A. Straus, and J. Xu, "Carbon nanotube - Silicon heterojunction arrays and infrared photocurrent responses", Journal of Physical Chemistry C, 111(15), 5800-5804, (2007) (ARO seed funding).
16. D. A. Straus, T.-F. Kuo, M. B. Tzolov, and J. Xu, "Photocurrent Response of the Carbon Nanotube - Silicon Heterojunction Array". IET Circuits, Devices & Systems, Special Issue on Quantum Dots and Nanowires, 1(3) 200-204, 2007. (ARO seed funding)
17. Yin, M. B. Tzolov, D. Cardimona, and J. Xu, "Fabrication of Highly Ordered Anodic Aluminum Oxide Template on Silicon Substrate", IET Circuits, Devices & Systems, 1(3), 205-209, 2007.
18. T. F. Kuo, D. A. Straus, M. B. Tzolov, and J. M. Xu, (invited) "Carbon Nanotube – Silicon Heterojunction Hyperspectral Photocurrent Response", Mater. Res. Soc. Symp. Proc., 963 0963-Q22-01, 2007.
19. Jimmy Xu, "Arrayed carbon nanotube – silicon heterojunction: a new IV-IV semiconductor system and uncooled IR sensing ", 2007 Workshop on Compound Semiconductors and ICs, Venice, Italy, May 20-23, 2007.

References

[1] http://www.mapoflife.org/topics/topic_312_Infrared-detection-in-snakes/.
[2] E. O. Gracheva*, et al.*, "Molecular basis of infrared detection by snakes," *Nature,* vol. 464, pp. 1006-U66, Apr 15 2010.
[3] A. Subrahmanyam*, et al.*, "Nano-vanadium oxide thin films in mixed phase for microbolometer applications," *Journal of Physics D-Applied Physics,* vol. 41, p. 195108, Oct 7 2008.
[4] F. Niklaus*, et al.*, "MEMS-Based Uncooled Infrared Bolometer Arrays – A Review," *Proc. SPIE 6836,* vol. 68360D, 2007.
[5] A. V. Kolobov*, et al.*, "Understanding the phase-change mechanism of rewritable optical media," *Nature Materials,* vol. 3, pp. 703-708, Oct 2004.
[6] F. J. Morin, "Oxides Which Show a Metal-to-Insulator Transition at the Neel Temperature," *Physical Review Letters,* vol. 3, pp. 34-36, 1959.
[7] K. C. Liddiard, "Thin-Film Resistance Bolometer Ir Detectors," *Infrared Physics,* vol. 24, pp. 57-64, 1984.
[8] Z. C. Wu*, et al.*, "Transparent, conductive carbon nanotube films," *Science,* vol. 305, pp. 1273-1276, Aug 27 2004.

[9] E. S. Snow*, et al.*, "Random networks of carbon nanotubes as an electronic material," *Applied Physics Letters,* vol. 82, pp. 2145-2147, Mar 31 2003.
[10] L. J. Hall*, et al.*, "Sign change of Poisson's ratio for carbon nanotube sheets," *Science,* vol. 320, pp. 504-507, Apr 25 2008.
[11] A. E. Aliev, "Bolometric detector on the basis of single-wall carbon nanotube/polymer composite," *Infrared Physics & Technology,* vol. 51, pp. 541-545, Oct 2008.
[12] M. E. Itkis*, et al.*, "Bolometric infrared photoresponse of suspended single-walled carbon nanotube films," *Science,* vol. 312, pp. 413-416, Apr 21 2006.
[13] R. T. Lu*, et al.*, "Suspending single-wall carbon nanotube thin film infrared bolometers on microchannels," *Applied Physics Letters,* vol. 94, p. 163110, Apr 20 2009.
[14] M. B. Jakubinek*, et al.*, "Temperature dependence of thermal conductivity enhancement in single-walled carbon nanotube/polystyrene composites," *Applied Physics Letters,* vol. 96, pp. 083105-083108 Feb 22 2010.
[15] D. H. Zhang*, et al.*, "Transparent, conductive, and flexible carbon nanotube films and their application in organic light-emitting diodes," *Nano Letters,* vol. 6, pp. 1880-1886, Sep 13 2006.
[16] N. F. Mott, *Conduction in non-crystalline materials*. Oxford
New York: Clarendon Press ;
Oxford University Press, 1987.
[17] P. Sheng*, et al.*, "Fluctuation-Induced Tunneling Conduction in Carbon-Polyvinylchloride Composites," *Physical Review Letters,* vol. 40, pp. 1197-1200, 1978.
[18] K. Yanagi*, et al.*, "Transport Mechanisms in Metallic and Semiconducting Single-Wall Carbon Nanotube Networks," *Acs Nano,* vol. 4, pp. 4027-4032, Jul 2010.
[19] H. G. Schild, "Poly (N-Isopropylacrylamide) - Experiment, Theory and Application," *Progress in Polymer Science,* vol. 17, pp. 163-249, 1992.
[20] K. Takahashi*, et al.*, "Swelling and deswelling kinetics of poly(N-isopropylacrylamide) gels," *Journal of Chemical Physics,* vol. 120, pp. 2972-2979, Feb 8 2004.
[21] M. Tarasov*, et al.*, "Carbon nanotube bolometers," *Applied Physics Letters,* vol. 90, pp. 163503-163506, Apr 16 2007.
[22] S. Barrau*, et al.*, "DC and AC conductivity of carbon nanotubes-polyepoxy composites," *Macromolecules,* vol. 36, pp. 5187-5194, Jul 15 2003.
[23] B. Pradhan*, et al.*, "Carbon nanotube - Polymer nanocomposite infrared sensor," *Nano Letters,* vol. 8, pp. 1142-1146, Apr 2008.
[24] B. R. Sankapal*, et al.*, "Electrical properties of air-stable, iodine-doped carbon-nanotube-polymer composites," *Applied Physics Letters,* vol. 91, pp. 173103-173106 Oct 22 2007.
[25] M. T. Connor*, et al.*, "Broadband ac conductivity of conductor-polymer composites," *Physical Review B,* vol. 57, pp. 2286-2294, Jan 15 1998.
[26] I. J. Suarez*, et al.*, "Swelling kinetics of poly(N-isopropylacrylamide) minigels," *Journal of Physical Chemistry B,* vol. 110, pp. 25729-25733, Dec 28 2006.